Modeling and Analysis of LEO Mega-Constellations as Nonhomogeneous Poisson Point Processes

Niloofar Okati and Taneli Riihonen
Faculty of Information Technology and Communication Sciences, Tampere University, Finland
e-mail: {niloofar.okati, taneli.riihonen}@tuni.fi

***Abstract*—Requirements and technological advancements towards 6th generation (6G) wireless networks lead to enabling and development of massive low Earth orbit (LEO) satellite constellations to provide ubiquitous and high-capacity connectivity, particularly for maritime and airborne platforms. Consequently, new methodologies to study the performance of LEO networks are of great importance. In this paper, we derive both downlink and uplink analytical expressions for coverage probability and data rate of a massive inclined LEO constellation under general shadowing and fading. We model the LEO satellite network as a nonhomogeneous Poisson point process with general intensity in order to take into account uneven distribution of satellites along the latitudes. The results provided in this study facilitate the stochastic evaluation and design of the future massive LEO networks, regardless of satellites' exact trajectories in orbits.**

I. Introduction

As 5th generation (5G) cellular networks are becoming fully commercial all around the globe, characterizing 6G challenges and requirements has recently attracted significant attention [1]–[3]. Providing ubiquitous and high-capacity connectivity, as promised in 6G, requires enabling and development of non-terrestrial networks. Among non-terrestrial networks low Earth orbit (LEO) satellite systems have gained increasing popularity due to providing seamless connectivity with lower round-trip delay—compared to geostationary satellites—especially for remote regions where the deployment of terrestrial networks is not economically reasonable [4], [5].

Despite the commercial promotion of massive LEO networks (e.g., Starlink, Kuiper, Telesat), there are still many unanswered questions regarding the performance and design of these networks. Literature around LEO systems' analysis is mostly limited to the analysis of few satellites with deterministic locations and coverage areas. The uplink outage probability in the presence of interference was evaluated for two LEO constellations through time-domain simulations in [6]. The effect of traffic non-uniformity was studied in [7] by assuming hexagonal service areas for satellites.

A general expression for a single LEO satellite's visibility time was provided in [8], but it is incapable of concluding the general distribution of visibility periods for any arbitrarily positioned user. The deterministic model in [8] was then developed via statistical analysis of coverage time in mobile LEO during a satellite visit [9]. In [10], the Doppler shift magnitude of a LEO network is characterized for a single spotbeam by using tools from stochastic geometry. Resource control of a hybrid satellite–terrestrial network was performed in [11] with two objectives of maximizing the delay-limited capacity and minimizing the outage probability. A hybrid satellite–terrestrial network to assist 5G infrastructure has been analyzed by considering only one spotbeam [12], [13]. In [14], the outage probability of a satellite-based IoT network, in which the LEO satellites relay the data to the ground stations, is derived in closed form by assuming a low number of satellites at the known locations.

Only recently, more research based on stochastic geometry of LEO networks has started emerging. In our seminal study [15], generic performance of satellite networking without resorting to explicit orbit simulations and the actual geometry of any specific constellation has been formulated by assuming uniform distribution for satellites. Due to the fact that satellites in practical constellations are distributed unevenly along different latitudes [16], i.e., the number of satellites on the inclination limits is greater than on equatorial regions, the density of practical deterministic constellations is typically not uniform. In [15], [16], we compensated for this mismatch by derivation of a new parameter called effective number of satellites. In [17], stochastic geometry is utilized to derive the coverage probability of a LEO network, where satellite gateways act as relays between the satellites and users. Unlike in [15], the satellites are assumed to be placed at different altitudes. The uplink communication scenario is characterized by considering interfering terrestrial transmitters in [18].

In this paper, downlink and uplink coverage probability and data rate of inclined LEO constellations are analyzed under a general shadowing and fading propagation model. Unlike in [15]–[17], the satellites' positions are assumed to be distributed as a nonhomogeneous Poisson point process (NPPP), which models the actual distribution of satellites along different latitudes more precisely by selecting the proper intensity. Finally, the mathematical expressions are verified through simulations and the main findings of this paper are demonstrated for different network parameters, e.g., altitude, inclination angle, user's latitude, and minimum elevation angle required for a satellite to be visible to the user.

The organization of the remainder of this paper is as follows. Section II describes the system model as well as the mathematical preliminaries for modeling a LEO network as an NPPP. Performance analysis of a LEO network in terms of coverage probability and average data rate is provided in Section III. This is followed by the numerical results in Section IV. Finally, the paper is concluded in Section V.

II. System Model

The studied network model in this paper is a massive LEO communication satellite constellation, as shown in Fig. 1, that consists of N satellites distributed uniformly on low circular orbits with inclination angle, ι, and altitude denoted by $r_{\min}$. The altitude parameter $r_{\min}$ has the peculiar subscript because it specifies also the minimum possible distance between a satellite and a user on Earth (that is realized when it is at the zenith). The satellites' coordinates in terms of their latitude and longitude are denoted by $(\phi_{\rm s}, \lambda_{\rm s})$.

User terminals are located on a specific latitude, denoted by $\phi_{\rm u}$, on the surface of Earth with radius $r_{\oplus} \approx 6371$ km. The wireless transmissions propagate to/from a user from/to all and only the satellites that are elevated above the horizon to an angle of $\theta_{\rm s} \geq \theta_{\min}$. Smaller values for $\theta_{\min}$ result in a more drastic path loss due to the greater distance between a user and a satellite. Correspondingly, $r_{\max}$ denotes the maximum possible distance at which a satellite and a user may be able to communicate without terrain blockage (that is realized when $\theta_{\rm s} = \theta_{\min}$):

$$\frac{r_{\max}}{r_{\oplus}} = \sqrt{\frac{r_{\min}}{r_{\oplus}}\left(\frac{r_{\min}}{r_{\oplus}} + 2\right) + \sin^2(\theta_{\min})} - \sin(\theta_{\min}). \quad (1)$$

We assume an association policy where the user communicates with its nearest satellite that is referred to as the serving satellite in what follows. The network performance can be considered as noise-limited due to implementing resource scheduling and co-channel interference mitigation properly. The distances from the user to the serving satellite and the other satellites are denoted by r_0 and r_n, $n = 1, 2, \ldots, N-1$, respectively, while G_0 and G_n represent the corresponding channel gains. Shadowing effect is modeled by the random variable $\mathcal{X}_n$, where $n = 0, 1, \ldots, N-1$. Obviously, $\mathcal{X}_n = G_n = 0$ if $r_n > r_{\max}$ for some $n = 0, 1, \ldots, N-1$.

Based on the described system model, the signal-to-noise ratio (SNR) at the receiver can be expressed as

$$\text{SNR} = \begin{cases} \dfrac{p_{\rm s} G_0 \mathcal{X}_0 r_0^{-\alpha}}{\sigma^2}, & r_0 \leq r_{\max}, \\ 0, & \text{otherwise}, \end{cases} \quad (2)$$

where $p_{\rm s}$ is the transmission power of the serving satellite. We assume that the user's receiver is subject to additive white Gaussian noise with constant power σ^2, and the parameter α is a path loss exponent.

In the satellite constellation described earlier, the satellites are distributed unevenly along different latitudes which means that there are more visible satellites for a user located close to inclination limits than for a user on equatorial region. In order to model the latitude-dependent distribution of satellites, we assume that N satellites are distributed according to an NPPP, ξ, on a sphere with radius $r_{\oplus} + r_{\min}$. The void probability on some bounded surface area $\mathcal{A}$ on the sphere is given by

$$\mathbb{P}(\xi(\mathcal{A}) = 0) \quad (3)$$
$$= \exp\left(-\iint_{\mathcal{A}} \delta(\phi_{\rm s}, \lambda_{\rm s})\,(r_{\min} + r_{\oplus})^2 \cos(\phi_{\rm s})\, d\phi_{\rm s} d\lambda_{\rm s}\right),$$

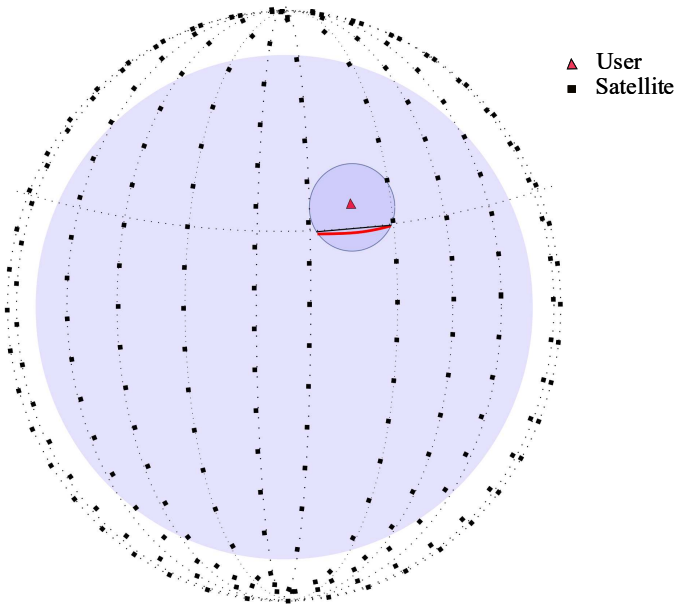

Fig. 1. System model for N satellites distributed uniformly over inclined orbits (polar orbits with $\iota = 90^\circ$ inclination in this example).

where $\delta(\phi_{\rm s}, \lambda_{\rm s})$ is the intensity function of the NPPP at latitude $\phi_{\rm s}$ and longitude $\lambda_{\rm s}$.

Lemma 1. *When satellites are distributed uniformly on low circular orbits with the same inclination angle, ι, and altitude, $r_{\min}$, the intensity function of the NPPP is given by*

$$\delta(\phi_{\rm s}) = \frac{N}{\sqrt{2}\pi^2 (r_{\min} + r_{\oplus})^2} \cdot \frac{1}{\sqrt{\cos(2\phi_{\rm s}) - \cos(2\iota)}}, \quad (4)$$

and we can denote $\delta(\phi_{\rm s}, \lambda_{\rm s}) = \delta(\phi_{\rm s})$ since it does not depend on $\lambda_{\rm s}$, for $\phi_{\rm s} \in [-\iota, \iota]$.

Proof. For any longitude $\lambda_{\rm s}$, the intensity function is equivalent to the actual density of the satellites on a sphere surface element at latitude $\phi_{\rm s}$ that can be written as

$$\delta(\phi_{\rm s}) = \frac{N f_{\Phi_{\rm s}}(\phi_{\rm s})\, d\phi_{\rm s}}{2\pi (r_{\min} + r_{\oplus})^2 \cos(\phi_{\rm s})\, d\phi_{\rm s}}, \quad (5)$$

where the nominator and denominator represent the number of satellites resided in the surface element and its surface area, respectively. Substituting the probability density $f_{\Phi_{\rm s}}(\phi_{\rm s})$ of random latitude $\Phi_{\rm s}$ [16, Lemma 2] completes the proof. □

III. Performance Analysis

In order to contribute expressions for coverage probability and average achievable rate, we model the satellite network as a nonhomogeneous Poisson point process with intensity given in Lemma 1. Towards this, we need first to characterize some basic distance distributions that stem from the geometry of the considered system model.

A. Distance to the Serving Satellite

We express the probability density function (PDF) of the distance to the nearest satellite in the following lemma. The

functions are required for the derivation of the studied performance metrics in the following subsections.

Lemma 2. *The PDF of the random serving distance R_0 when the satellites are distributed according to a nonhomogeneous PPP with intensity $\delta(\phi_\mathrm{s}, \lambda_\mathrm{s})$, is given by*

$$f_{R_0}(r_0) = 2r_0\left(\frac{r_{\min}}{r_\oplus}+1\right)\int_{\max(\phi_\mathrm{u}-\theta_0,-\iota)}^{\min(\phi_\mathrm{u}+\theta_0,\iota)} \delta(\phi_\mathrm{s})\cos(\phi_\mathrm{s}) \times \frac{1}{\sqrt{\cos^2(\phi_\mathrm{s}-\phi_\mathrm{u})-\cos^2(\theta_0)}}d\phi_\mathrm{s} \times \exp\left(-2(r_{\min}+r_\oplus)^2\int_{\max(\phi_\mathrm{u}-\theta_0,-\iota)}^{\min(\phi_\mathrm{u}+\theta_0,\iota)}\delta(\phi_\mathrm{s})\cos(\phi_\mathrm{s}) \times \cos^{-1}\left(\frac{\cos(\theta_0)}{\cos(\phi_\mathrm{s}-\phi_\mathrm{u})}\right)d\phi_\mathrm{s}\right) \quad (6)$$

for $r_0 \in [r_{\min}, 2r_\oplus + r_{\min}]$ while $f_{R_0}(r_0) = 0$ otherwise. The polar angle difference between the serving satellite and the user is $\theta_0 = \cos^{-1}\left(1 - \frac{r_0^2 - r_{\min}^2}{2(r_{\min}+r_\oplus)r_\oplus}\right)$.

Proof. For a nonhomogeneous PPP, the CDF of R_0 can be written as

$$F_{R_0}(r_0) = 1 - \mathbb{P}(R_0 > r_0) = 1 - \mathbb{P}(\xi(\mathcal{A}) = 0) \quad (7)$$

where $\mathbb{P}(\xi(\mathcal{A}) = 0)$ is the void probability of PPP given in (3) and $\mathcal{A}$ is the shaded cap above the user shown in Fig. 1. According to (3), by integrating from the intensity over the spherical cap above the user, we have

$$\begin{aligned} F_{R_0}(r_0) &= 1 - \exp\left(-\int_{\max(\phi_\mathrm{u}-\theta_0,-\iota)}^{\min(\phi_\mathrm{u}+\theta_0,\iota)}\beta(\phi_\mathrm{s})\delta(\phi_\mathrm{s})(r_{\min}+r_\oplus)^2\cos(\phi_\mathrm{s})d\phi_\mathrm{s}\right) \\ &\overset{(a)}{=} 1 - \exp\left(-2(r_{\min}+r_\oplus)^2\int_{\max(\phi_\mathrm{u}-\theta_0,-\iota)}^{\min(\phi_\mathrm{u}+\theta_0,\iota)}\delta(\phi_\mathrm{s})\cos(\phi_\mathrm{s}) \times \cos^{-1}\left(\frac{\cos(\theta_0)}{\cos(\phi_\mathrm{s}-\phi_\mathrm{u})}\right)d\phi_\mathrm{s}\right), \end{aligned} \quad (8)$$

where $\beta(\phi_\mathrm{s})$ is the longitude range of the red surface element in Fig. 1 and (a) follows from substitution of $\beta(\phi_\mathrm{s})$ using the basic geometry. Taking the derivative of (8) with respect to r_0 completes the proof of Lemma 2. □

Lemma 3. *The PDF of the serving distance R_0 when the satellites are distributed uniformly with constant intensity $\delta = \frac{N}{4\pi(r_{\min}+r_\oplus)^2}$, is given by*

$$f_{R_0}(r_0) = \frac{Nr_0}{2r_\oplus(r_{\min}+r_\oplus)}\exp\left(-N\left(\frac{r_0^2-r_{\min}^2}{4r_\oplus(r_{\min}+r_\oplus)}\right)\right) \quad (9)$$

for $r_0 \in [r_{\min}, 2r_\oplus + r_{\min}]$ while $f_{R_0}(r_0) = 0$ otherwise.

Proof. The proof follows the same principles as the proof of Lemma 2. However, the integration from a constant density over the cap will reduce to a simple expression. Thus, $F_{R_0}(r_0) = 1 - \exp\left(-N\left(\frac{r_0^2-r_{\min}^2}{4r_\oplus(r_{\min}+r_\oplus)}\right)\right)$. Taking the derivative of the CDF with respect to r_0 completes the proof. □

B. Coverage Probability and Average Data Rate

The following performance analysis in terms of coverage probability and average data rate holds for both downlink and uplink communication directions. Furthermore, it is presented under general shadowing and fading distributions so that any specific scenario can be covered by appropriate choice of $f_{\mathcal{X}_0}(x_0)$ and $F_{G_0}(g_0)$, respectively, e.g., Rician fading with lognormal shadowing in our numerical results.

Let us first derive the coverage probability of the LEO satellite network for a user in an arbitrary location on Earth. The performance measure of coverage probability is defined as the probability of having at least the minimum SNR required for successful data transmission. Thus, the coverage probability is defined as

$$P_\mathrm{c}(T) \triangleq \mathbb{P}(\mathrm{SNR} > T) = \mathbb{P}\left(\frac{p_\mathrm{s}G_0R_0^{-\alpha}}{\sigma^2} > T\right), \quad (10)$$

where σ^2 is additive noise with constant power, and α represents exponent of path loss.

Proposition 1. *The probability of coverage for an arbitrarily located user under general shadowing and fading is*

$$P_\mathrm{c}(T) \triangleq \mathbb{P}(\mathrm{SNR} > T) = \int_{r_{\min}}^{r_{\max}}\int_0^\infty f_{\mathcal{X}_0}(x_0)f_{R_0}(r_0)\left(1 - F_{G_0}\left(\frac{Tr_0^\alpha\sigma^2}{p_\mathrm{s}x_0}\right)\right)dx_0dr_0, \quad (11)$$

where $f_{R_0}(r_0)$ is given in Lemma 2 or Lemma 3 and $f_{\mathcal{X}_0}(x_0)$ is the PDF of $\mathcal{X}_0$.

Proof. To obtain (11), we start with the definition of coverage probability:

$$\begin{aligned} P_\mathrm{c}(T) &= \mathbb{E}_{R_0}\left[\mathbb{P}(\mathrm{SNR} > T|R_0)\right] \\ &= \int_{r_{\min}}^{r_{\max}}\mathbb{P}(\mathrm{SNR} > T|R_0 = r_0)f_{R_0}(r_0)dr_0 \\ &= \int_{r_{\min}}^{r_{\max}}\mathbb{P}\left(G_0\mathcal{X}_0 > \frac{Tr_0^\alpha\sigma^2}{p_\mathrm{s}}\right)f_{R_0}(r_0)dr_0. \end{aligned} \quad (12)$$

The upper limit for the integral is due to the fact that the satellites with smaller than $\theta_{\min}$ elevation angle have no visibility to the user. The proof is completed by substitution of the product distribution of two independent random variables in (12). □

The average achievable data rate (in bit/s/Hz) of an arbitrary user over generalized fading channels and shadowing can be derived in the following proposition.

Proposition 2. *The average rate (in bits/s/Hz) of an arbitrarily located user and its serving satellite under general shadowing and fading assumption is*

$$\bar{C} \triangleq \mathbb{E}\left[\log_2(1+\mathrm{SNR})\right] = \frac{1}{\ln(2)}\int_{r_{\min}}^{r_{\max}}\int_0^\infty\int_0^\infty f_{\mathcal{X}_0}(x_0)\left(1 - F_{G_0}\left(\frac{r_0^\alpha\sigma^2}{p_\mathrm{s}}\left(e^t-1\right)\right)\right) \times f_{R_0}(r_0)dx_0dtdr_0. \quad (13)$$

TABLE I
SIMULATION PARAMETERS

Parameters	Values
Path loss exponent, α	2
Rician factor, K	100
Transmission power, $p_{\rm s}$ (W)	10
Noise power, σ^2 (dBm)	-103
User's latitude, $\phi_{\rm u}$ (degrees)	61.5
Mean and standard deviation of lognormal distribution: $\mu_{\rm s}$ (dB), $\sigma_{\rm s}$ (dB)	0, 9

Proof. Taking the expectation over serving distance and channel gain, we have

$$\begin{aligned}\bar{C} &= \mathbb{E}_{G_0,\mathcal{X}_0,R_0}\left[\log_2\left(1+\mathrm{SNR}\right)\right]\\ &= \frac{1}{\ln(2)}\int_{r_{\min}}^{r_{\max}} \mathbb{E}\left[\ln\left(1+\frac{p_{\rm s}G_0\mathcal{X}_0 r_0^{-\alpha}}{\sigma^2}\right)\right] f_{R_0}(r_0)\,dr_0\\ &\overset{(a)}{=} \frac{1}{\ln(2)}\int_{r_{\min}}^{r_{\max}}\int_0^{\infty} \mathbb{P}\left[\ln\left(1+\frac{p_{\rm s}G_0\mathcal{X}_0 r_0^{-\alpha}}{\sigma^2}\right)>t\right] f_{R_0}(r_0)\,dt dr_0\\ &= \frac{1}{\ln(2)}\int_{r_{\min}}^{r_{\max}}\int_0^{\infty} \mathbb{P}\left[G_0\mathcal{X}_0 > \frac{r_0^{\alpha}\sigma^2}{p_{\rm s}}\left(e^t-1\right)\right] f_{R_0}(r_0)\,dt dr_0,\end{aligned} \tag{14}$$

where (a) follows from the fact that for a positive random variable X, $\mathbb{E}[X]=\int_{t>0}\mathbb{P}(X>t)\,dt$. □

IV. NUMERICAL RESULTS

In this section, we corroborate our analytical findings through Monte Carlo simulations. The propagation model takes into account the large-scale attenuation with path loss exponent $\alpha = 2$, the small-scale Rician fading with parameter $K = 100$, and lognormal shadowing. As a result, the corresponding channel gains, G_n, (being the square of the Rice random variable) have a noncentral chi-squared distribution, χ^2, with two degrees of freedom and non-centrality parameter $2K$. Therefore, the CDF in Propositions 1 and 2 is $F_{G_0}(g_0) = 1 - Q_1\left(\sqrt{2K}, \sqrt{g_0}\right)$, where $Q_1(\cdot,\cdot)$ denotes the Marcum Q-function. The lognormal shadowing is represented as $\mathcal{X}_0 = 10^{X_0/10}$ such that $X_0 \sim \mathcal{N}(\mu_{\rm s}, \sigma_{\rm s})$, where $\mathcal{N}$ is a normal distribution with $\mu_{\rm s}$ and $\sigma_{\rm s}$ being its mean and standard deviation in decibels. Thus, the PDF of lognormal shadowing is $f_{\mathcal{X}_0}(x_0) = \frac{10}{\ln(10)\sqrt{2\pi}\sigma_{\rm s}x_0}\exp\left(-\frac{1}{2}\left(\frac{10\log_{10}(x_0)-\mu_{\rm s}}{\sigma_{\rm s}}\right)^2\right)$. The simulation parameters are given in Table I.

Figure 2 verifies the coverage expression given in Proposition 1, considering different altitudes for $N = 648$ and $\iota = 90°$. The user is assumed to be at Tampere, Finland ($\phi_{\rm u} = 61.5°$). As shown in Fig. 2, the simulation results (markers) are perfectly matched with the analytical expression (lines) given in Proposition 1. With increasing the altitude, coverage decreases accordingly due to more drastic path loss for larger distances. The effect of shadowing on coverage probability is ambiguous. As it is shown in the figure, as the chance of the user being in outage increases, shadowing affects the coverage probability more positively, the reason being that shadowing randomness increases the chance of a user with poor SNR to be in coverage. It can be also interpreted that user association techniques based on maximum received signal are able to considerably improve the coverage probability.

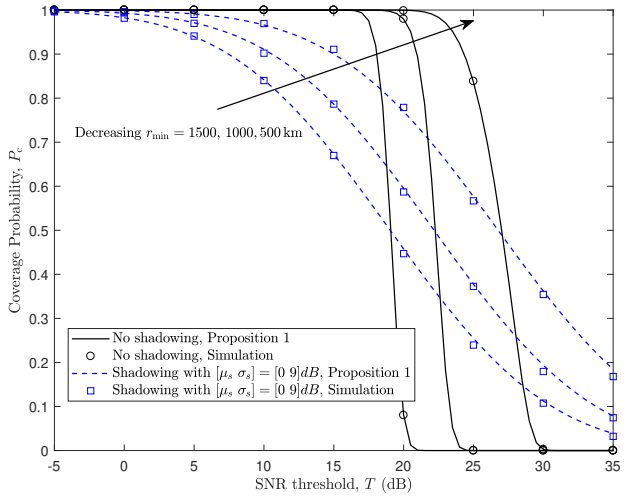

Fig. 2. Verification of Proposition 1 with simulations when $K = 100$, $\iota = 90°$, $r_{\min} \in \{500, 1000, 1500\}$ km, $\phi_{\rm u} = 61.5°$, and $\theta_{\min} = 10°$.

Validation of data rate given by Proposition 2 is shown in Fig. 3 for different minimum elevation angles. The data rate decreases with increasing the minimum elevation angle due to a reduction in the chance of satellite visibility to the user. For smaller values of $\theta_{\min}$, the data rate increases by decreasing the altitude due to the reduction in path loss. However, as $\theta_{\min}$ increases, the higher altitudes result in a higher data rate since the visibility probability increases by rising the altitude.

Coverage probability and data rate versus altitude for different users' latitudes, satellites' inclination angles, and minimum required elevation angles are depicted in Figs. 4 and 5, respectively. Starting from very low altitudes, coverage probability and data rate improve with increasing the altitude since a better chance of line-of-sight is attained for the serving satellite which is then followed by a decline caused by more severe path loss in higher altitudes. In both plots, the optimum altitude increases with rising the minimum elevation angle while the maximum achieved coverage and rate decrease accordingly. Moreover, smaller inclination angles result in a superior performance due to the higher density of satellites and, therefore, the existence of a stronger serving channel.

V. CONCLUSIONS

In this paper, we studied the performance of low Earth orbit satellite networks in a more generic form comparing with the existing literature on this topic. The satellite network is modeled as a nonhomogeneous Poisson point process which models the uneven distribution of satellites along different latitudes with its intensity being a function of satellites' actual distributions. Utilizing such a model for satellites' locations facilitates derivation of the coverage probability and data rate of an arbitrary user under general fading and shadowing. The proposed analysis paves the way for a more reliable integration of the LEO networks and the existing cellular network in 6G.

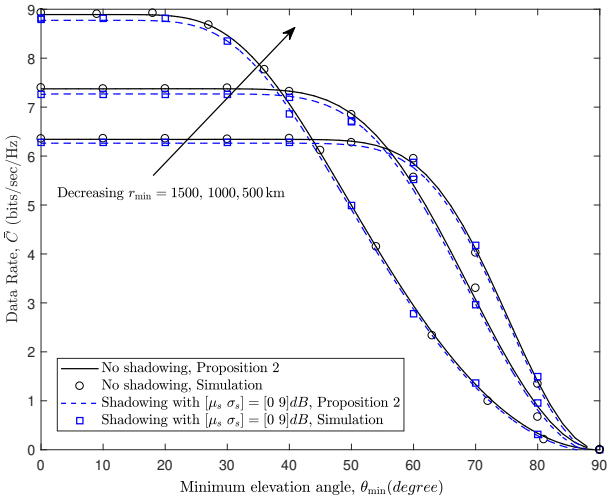

Fig. 3. Verification of Proposition 2 with simulations when $K = 100$, $\iota = 90°$, $r_{\min} \in \{500, 1000, 1500\}$ km, $\phi_{\mathrm{u}} = 61.5°$, and $\theta_{\min} = 10°$.

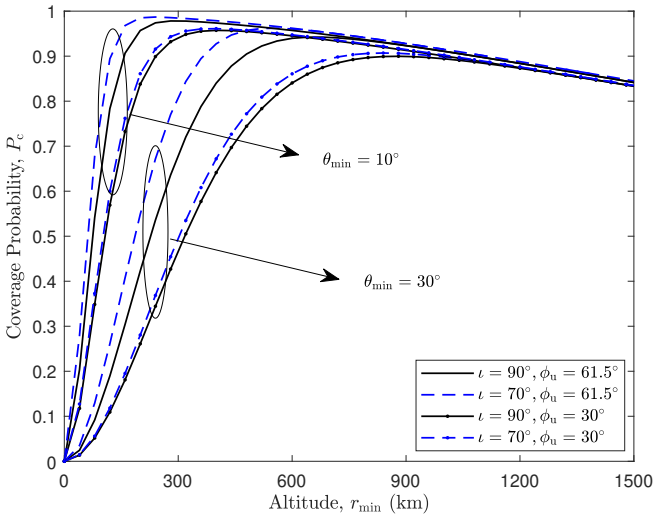

Fig. 4. Coverage probability for different altitudes when $K = 100$, $T = 10$ dB, and $\iota = \{90°, 70°\}$.

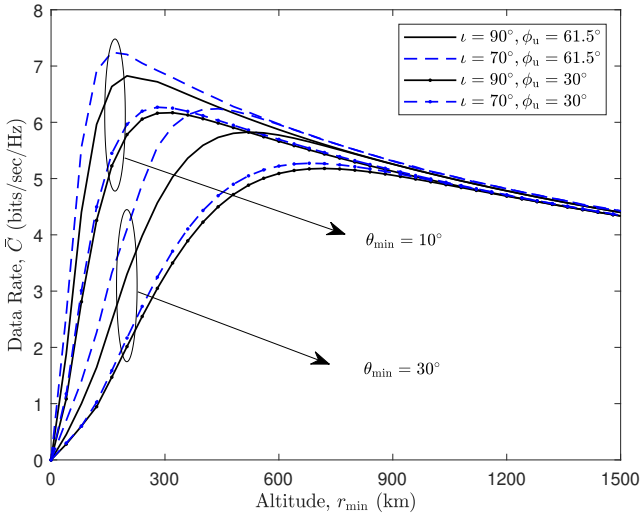

Fig. 5. Data rate for different altitudes when $K = 100$ and $\iota = \{90°, 70°\}$.

ACKNOWLEDGMENT

This research work was supported by a Nokia University Donation.

REFERENCES

[1] M. Giordani and M. Zorzi, "Non-terrestrial communication in the 6G era: Challenges and opportunities," *available online: https://arxiv.org/abs/1912.10226v2*, 2019.

[2] Z. Jia, M. Sheng, J. Li, D. Zhou, and Z. Han, "Joint HAP access and LEO satellite backhaul in 6G: Matching game based approaches," *IEEE Journal on Selected Areas in Communications*, Aug. 2020.

[3] M. Giordani, M. Polese, M. Mezzavilla, S. Rangan, and M. Zorzi, "Toward 6G networks: Use cases and technologies," *IEEE Communications Magazine*, vol. 58, no. 3, pp. 55–61, Mar. 2020.

[4] J. L. Grubb, "The traveler's dream come true," *IEEE Communications Magazine*, vol. 29, no. 11, pp. 48–51, Nov. 1991.

[5] A. Mokhtar and M. Azizoglu, "On the downlink throughput of a broadband LEO satellite network with hopping beams," *IEEE Communications Letters*, vol. 4, no. 12, pp. 390–393, Dec. 2000.

[6] F. Vatalaro, G. E. Corazza, C. Caini, and C. Ferrarelli, "Analysis of LEO, MEO, and GEO global mobile satellite systems in the presence of interference and fading," *IEEE Journal on Selected Areas in Communications*, vol. 13, no. 2, pp. 291–300, Feb. 1995.

[7] H. M. Mourad, A. A. M. Al-Bassiouni, S. S. Emam, and E. K. Al-Hussaini, "Generalized performance evaluation of low Earth orbit satellite systems," *IEEE Communications Letters*, vol. 5, no. 10, pp. 405–407, Oct. 2001.

[8] I. Ali, N. Al-Dhahir, and J. E. Hershey, "Predicting the visibility of LEO satellites," *IEEE Transactions on Aerospace and Electronic Systems*, vol. 35, no. 4, pp. 1183–1190, Oct. 1999.

[9] Y. Seyedi and S. M. Safavi, "On the analysis of random coverage time in mobile LEO satellite communications," *IEEE Communications Letters*, vol. 16, no. 5, pp. 612–615, May 2012.

[10] T. A. Khan and M. Afshang, "A stochastic geometry approach to Doppler characterization in a LEO satellite network," in *IEEE International Conference on Communications (ICC)*, Jun. 2020.

[11] J. Hu, G. Li, D. Bian, L. Gou, and C. Wang, "Optimal power control for cognitive LEO constellation with terrestrial networks," *IEEE Communications Letters*, vol. 24, no. 3, pp. 622–625, Mar. 2020.

[12] J. Zhang, B. Evans, M. A. Imran, X. Zhang, and W. Wang, "Performance analysis of C/U split hybrid satellite terrestrial network for 5G systems," in *20th IEEE International Workshop on Computer Aided Modelling and Design of Communication Links and Networks (CAMAD)*, Sep. 2015.

[13] A. J. Roumeliotis, C. I. Kourogiorgas, and A. D. Panagopoulos, "Optimal dynamic capacity allocation for high throughput satellite communications systems," *IEEE Wireless Communications Letters*, vol. 8, no. 2, pp. 596–599, Apr. 2019.

[14] A. K. Dwivedi, S. P. Chokkarapu, S. Chaudhari, and N. Varshney, "Performance analysis of novel direct access schemes for LEO satellites based IoT network," in *Proc. IEEE 31st Annual International Symposium on Personal, Indoor and Mobile Radio Communications*, Sep. 2020.

[15] N. Okati, T. Riihonen, D. Korpi, I. Angervuori, and R. Wichman, "Downlink coverage and rate analysis of low Earth orbit satellite constellations using stochastic geometry," *IEEE Transactions on Communications*, vol. 68, no. 8, pp. 5120–5134, Aug. 2020.

[16] N. Okati and T. Riihonen, "Stochastic analysis of satellite broadband by mega-constellations with inclined LEOs," in *Proc. IEEE 31st Annual International Symposium on Personal, Indoor and Mobile Radio Communications*, Sep. 2020.

[17] A. Talgat, M. A. Kishk, and M. S. Alouini, "Stochastic geometry-based analysis of LEO satellite communication systems," in *Proc. IEEE Communications Letters*, Oct. 2020.

[18] A. Yastrebova, I. Angervuori, N. Okati, M. Vehkaperä, M. Höyhtyä, R. Wichman, and T. Riihonen, "Theoretical and simulation-based analysis of terrestrial interference to LEO satellite uplinks," in *Proc. IEEE Global Communications Conference (GLOBECOM)*, Dec. 2020.